

**Experimental search for the bound-state singlet deuteron in the radiative  $n$ - $p$  capture**T. Belgya,<sup>1</sup> S. B. Borzakov,<sup>2</sup> M. Jentschel,<sup>3</sup> B. Maroti,<sup>1</sup> Yu. N. Pokotilovski,<sup>2,\*</sup> and L. Szentmiklosi<sup>1</sup><sup>1</sup>Centre for Energy Research, Hungarian Academy of Sciences, H-1525 Budapest 114, P.O. Box 49, Hungary<sup>2</sup>Joint Institute for Nuclear Research 141980 Dubna, Moscow Region, Russia<sup>3</sup>Institut Laue-Langevin, BP 156, 38042 Cedex 9 Grenoble, France

(Received 21 October 2018; published 17 April 2019)

We performed an experimental search for the bound-state singlet deuteron predicted in some microscopic calculations. The predicted energy of this metastable level is in the vicinity of the deuteron disintegration threshold. This state should manifest itself in a two-photon transition following thermal neutron capture by protons. The experiment consists in the search for the second  $\gamma$  ray in the cascade through a high-statistics measurement of  $\gamma$ -ray spectra after cold neutron capture by hydrogen nuclei. The upper limit  $2\mu\text{b}$  ( $2\sigma$  level) is obtained for the cross section of the singlet deuteron production with the binding energy in the range 10–125 keV.

DOI: [10.1103/PhysRevC.99.044001](https://doi.org/10.1103/PhysRevC.99.044001)**I. INTRODUCTION**

A singlet deuteron ( $S = 0$ ,  $T = 1$ ) is usually considered as not bound, but as a virtually bound (“antibound,” “quasi-bound”) state with binding energy  $B < 0$ , indicating an unstable configuration.

As was shown theoretically [1,2] (see also the review [3]), existence of a bound state in a deuteron is strongly connected with the sign of the neutron-proton scattering length: If the scattering length is positive, there is a bound state; in the opposite case, if the scattering length is negative, there is no bound state. As is well known, the experimental values for the neutron-proton scattering lengths are following: the triplet scattering length  $b_+ = 10.82$  fm and the singlet scattering length  $b_- = -47.42$  fm [4].

Many experiments were devoted to searching for the singlet deuteron state (denoted as  $d^*$ ) in different nuclear reactions.

Cohen *et al.* [5,6] observed singlet deuterons in the reaction  ${}^9\text{Be}(p, d^*){}^8\text{Be}$  at the energy of incident protons, 12 MeV. Bohne *et al.* observed the analogous process in the reaction  ${}^3\text{He}({}^{10}\text{B}, d^*){}^{11}\text{C}$  [7]. Gaiser *et al.* [8] investigated the reaction  ${}^4\text{He}(d, p\alpha)n$  at the energy of bombarding deuterons, 7 MeV. Their data gave clear evidence for the production of the unbound singlet deuteron  $d^*$ .

Bochkarev *et al.* [9] investigated decays of excited  $2^+$  states of the  ${}^6\text{He}$ ,  ${}^6\text{Li}$ , and  ${}^6\text{Be}$  nuclei. From the energy and momentum conservation, the narrow peaks in the  $\alpha$  spectra were considered as indications of the two-particle decays: an  $\alpha$  particle and the singlet deuteron in the case of  ${}^6\text{Li}$  and an  $\alpha$  particle and the dineutron in the case of  ${}^6\text{He}$ . Interpretation of the experimental spectra in terms of the two-nucleon final-state interaction have led to an abnormally large nucleon-nucleon scattering length  $\approx 50$ –100 fm.

Generally, the problem of existence of the singlet deuteron is closely connected to the old problem of existence of the dineutron and more generally of the neutral nuclei.

Experimental search for the dineutron was the subject of a number of experiments [10]. In some of them, there were indications of observation of the dineutron, the tetra-neutron [11], and even multineutrons with the number of neutrons  $n \geq 6$  [12].

**II. THEORETICAL INDICATIONS**

Over the years, claims (based on microscopic calculations) have appeared that the binding energy of the  $np$  pair in the singlet state may be positive; the singlet deuteron is stable in respect to decay to the neutron and proton.

Maltman and Isgur [13] described the  $np$  system as the six-quark state; they have obtained  $400 \pm 400$  keV binding energy for the singlet state and 2.9 MeV for the triplet state.

Ivanov *et al.* [14] considered the deuteron as the Cooper  $np$  pair in the field-theoretical approach developed within Nambu-Jona-Lasinio model of light nuclei. They computed a binding energy of  $\epsilon_S = 79 \pm 12$  keV for the deuteron singlet state modeled as a Cooper pair in the  ${}^1S_0$  state and calculated the  $S$ -wave  $np$  scattering length in terms of the binding energy. The calculations agree well with the energy of the virtual level  $\epsilon_S = 74$  keV, defined from the experimental  $S$ -wave scattering length.

Hackenburg [15] employed the intermediate off-shell singlet and triplet deuterons treated as dressed dibaryons in his calculations. In a simple extension of the effective range theory, he predicted the existence of the singlet deuteron bound state. The binding energy of this singlet level was predicted to be  $E_S = 66$  keV. He showed that the radiative capture leads to the possibility of observing the metastable singlet level in the resonance scattering of  $\gamma$  quanta by deuterons and in two-photon radiative capture, with the expected cross section

\*pokot@nf.jinr.ru

for the latter being  $27 \mu\text{b}$ , more than four orders of magnitude less than the main  $np$  radiative capture channel.

Calculations of Yamazaki *et al.* [16] in the quenched lattice quantum chromodynamics lead to the conclusion that not only the triplet but also the singlet deuteron state should be bound.

It is also possible to use the idea of negative resonance instead of the virtual level [3,17,18] as a phenomenological model for the  $np$  scattering. Shapiro *et al.* [19] used this approach to describe the radiative capture reaction  $n(^3\text{He}, ^3\text{H})p$ . It was confirmed in the proton-tritium scattering experiment of Gibbons *et al.* [20].

In Ref. [17], it was assumed that the imaginary part of the scattering amplitude corresponds to the radiative resonance width. This model can also treat the scattering and the radiative capture. According to this model, the resonance width is of the order 10 eV, and the bound-state singlet deuteron may be observed in the resonance  $\gamma$ -ray scattering by deuterons or in the radiative  $^1\text{H}(n, \gamma)$  capture.

However, it is known from classic works [1–3] that the interpretation of the above calculations implies the existence of a bound spin-singlet deuteron, which is incorrect; the  $s$ -wave  $np$ -singlet scattering length is negative, which signals the existence of a virtual spin-singlet deuteron, not a bound state. Nevertheless, we decided to perform an experimental search for the bound-state singlet deuteron in the thermal neutron-proton radiative capture experiment.

### III. EXPERIMENT

To search for the bound-state singlet deuteron  $\gamma$ -ray pulse-height spectra were recorded from radiative neutron capture by protons. Existence of the bound-state singlet deuteron could be evidenced by a two-step  $\gamma$ -ray transition  $^3S_1$  (continuum)  $\rightarrow$   $^1S_0$  (metastable)  $\rightarrow$   $^3S_1$  (ground state) in addition to the direct one  $^1S_0 \rightarrow$   $^3S_1$  with energy 2223 keV. Our main interest was concentrated in the energy range  $\approx 100$  keV below the  $\gamma$  ray with  $E = 2223$  keV.

Preliminary experiments performed at the Dubna pulse reactor IBR-2 are described in Refs. [21,22]. We decided to carry out a measurement using higher neutron flux with lower background.

The experiment was performed at the cold neutron Prompt Gamma Activation Analysis (PGAA) facility of the Budapest Neutron Center [23]. The beam of cold neutrons was extracted from the cold source of the reactor, transported through a long curved neutron guide, and passed to the target in an evacuated flight tube. The neutron beam cross section on the target was  $2 \times 2$  cm<sup>2</sup>; the average thermal equivalent neutron flux at the sample position was about  $5 \times 10^7$  cm<sup>-2</sup> s<sup>-1</sup>. The sample chamber was  $10 \times 17 \times 22$  cm<sup>3</sup>. The flight tube and the target chamber were lined inside with a slow neutron absorber made from a <sup>6</sup>Li-containing plastic sheet. The target materials in our experiments were polyethylene and water. The polyethylene target was located between two  $\gamma$ -ray detectors: a BGO-shielded Compton-suppressed  $n$ -type coaxial HPGe detector of diameter  $50 \times 76$  mm<sup>3</sup> and a low-energy HPGe detector of diameter  $35.7 \times 15$  mm<sup>3</sup>. In the case of a water target, only the BGO-shielded Compton-suppressed  $n$ -type coaxial HPGe detector was used. The targets were seen by the detectors

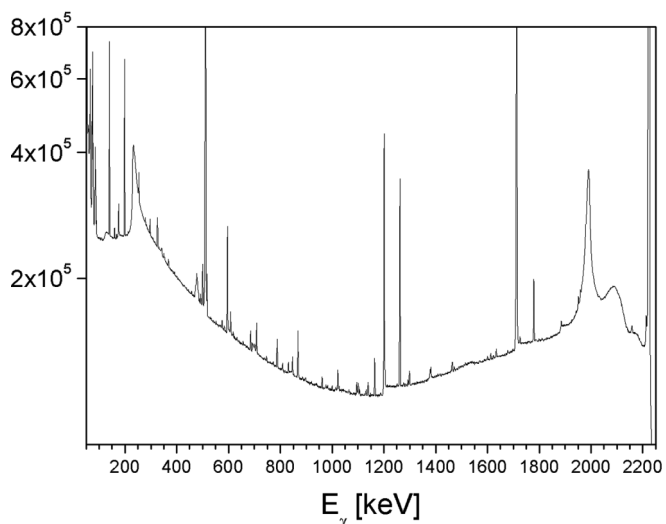


FIG. 1. Part of the  $\gamma$ -ray spectrum (50–2400 keV) of the coaxial HPGe detector measured with the polyethylene target.

through the lead collimators. The distance between the target center and the coaxial Ge detector was 23.5 cm and that between the target center and the low-energy Ge detector was 16 cm. The total measuring time was about 120 h for each of these targets. The values of the peak area of the main  $\text{H}(n, \gamma)\text{D}$  transition are as follows: With the coaxial detector and the polyethylene target it was measured as  $S(2223) = 3.8 \times 10^8$ ; with the low-energy detector,  $3.7 \times 10^7$ ; and with the coaxial detector and water target,  $1.45 \times 10^8$ . Background spectra were acquired with a graphite target and without any target as well.

### IV. REDUCTION OF DATA

Figure 1 shows the part of the spectrum of the HPGe coaxial detector in the energy range 50–2400 keV measured with the polyethylene target.

The most powerful peaks at the energy of 2223.25 keV ( $np$  capture  $\gamma$ -ray), its single- and double-escape peaks at the energies of 1712 and 1201 keV respectively and the positron annihilation peak at the energy of 511 keV, are accompanied by many peaks caused by the background of  $\gamma$  rays generated in the detector itself and materials surrounding the target and detectors.

An energy calibration procedure was used for finding a correspondence between the peak positions in the spectrum and energies of  $\gamma$  rays. As a calibration curve, we used a polynomial of third order consisting of terms having as parameters the coefficients of the energy calibration curve. The least squares method [24] was used to determine coefficients of the calibration polynomial. Then 22  $\gamma$  peaks arising from neutron capture by hydrogen and nuclei of isotopes of Ge, <sup>35</sup>Cl, <sup>12</sup>C, <sup>14</sup>N, <sup>27</sup>Al, and <sup>207</sup>Pb present in the spectrum were used for the calibration in the energy range from 50 keV to 11 MeV. Their energy values were taken from the NNDC and IAEA databases [25].

The  $\gamma$ -ray spectrum analysis programs VACTIV [26] and GENIE [27] have been used to obtain some of the peak areas in the measured spectra. These programs give contradictory results for the low-intensity peaks; the latter were analyzed with the MINUIT program [24].

Figures 2–4 show parts of the measured spectra in vicinity of the main  $n(p, D)\gamma$  transition in the 2100- to 2210-keV energy range.

Figure 2 presents the spectrum measured using the polyethylene target with the coaxial HPGe detector.

The peak doublets with energies of 2156.4 and 2158.9 keV have special interest. Their intensities are  $\approx 0.44 \times 10^{-4}$  and  $\approx 0.8 \times 10^{-4}$  respectively relative to the main 2223-keV peak. A possible interpretation of these peaks could be a 2156.3-keV  $\gamma$  line in  $^{36}\text{Cl}$  and a 2159.1-keV line in  $^{56}\text{Mn}$ , but their measured intensities are more than an order of magnitude larger than it would follow (2.3% and 1.4% respectively) from the ratio of the detected (more intense) lines in these nuclei after thermal neutron capture in  $^{35}\text{Cl}$  and  $^{55}\text{Mn}$  [25]. There was no other reasonable identification for these  $\gamma$  rays in prompt [25] or in radioactive [28]  $\gamma$ -ray transition databases. Therefore, at least one of these peaks could be considered as a candidate for a second  $\gamma$  ray in the searched for a two-step  $\gamma$ -ray transition  $^3\text{S}_1(\text{cont.}) \rightarrow ^1\text{S}_0(\text{metastable}) \rightarrow ^3\text{S}_1(\text{ground state})$ .

Figure 3 shows the same part of the spectrum of the low-energy planar HPGe detector measured with the polyethylene target.

This spectrum contains a number of interpreted weak peaks (see below) but neither of two peaks (2156.4 and 2158.9 keV) was found in the spectrum of the low-energy detector having (due to an order of magnitude lower background) sensitivity to weak peaks in this energy range not much worse than the coaxial detector. Therefore, we consider these peaks as due to  $\gamma$  rays coming from the surrounding of the coaxial detector or originating in the detector itself.

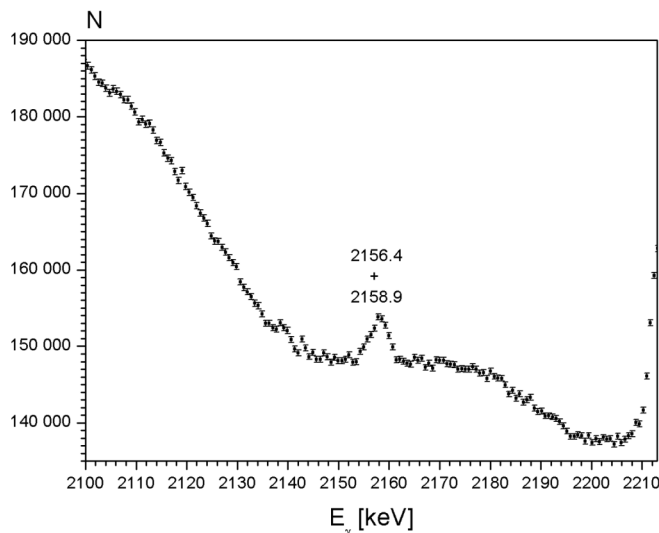


FIG. 2. Part of the  $\gamma$ -ray spectrum (2100–2210 keV) of the coaxial HPGe detector measured with the polyethylene target.

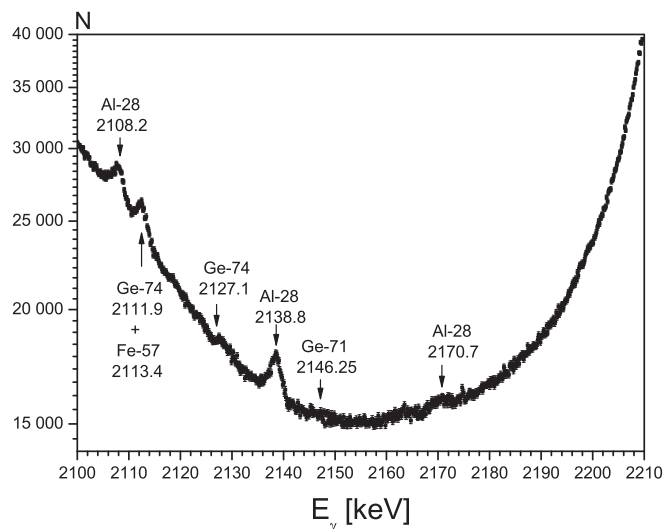


FIG. 3. Part of the  $\gamma$ -ray spectrum (2100–2210 keV) of the low-energy HPGe detector measured with the polyethylene target.

The main difficulty in the interpretation of the experimental spectra was caused by the background of  $\gamma$  rays generated in detectors and material surrounding the target and the detectors. Numerous peaks from neutron capture by isotopes of Ge, Cl, Fe, and by nuclei  $^{27}\text{Al}$ ,  $^{12}\text{C}$ ,  $^{14}\text{N}$  etc. have been observed in all measured spectra. We detected  $\approx 250$  peaks in the total spectrum up to 11 MeV.

From the area of the photopeak with  $E = 2223$  keV,  $S = 3.8 \times 10^8$  measured with the polyethylene target, known photo-peak efficiency  $1.9 \times 10^{-4}$  at this energy and distance from the target to the detector, and the ratio of the cold neutron-proton scattering to capture cross sections ( $\approx 50$  b/0.8 b  $\approx 60$ ), we estimate the total number of cold neutrons scattered by the polyethylene target as  $\approx 2 \times 10^{14}$ . From the areas of numerous  $\gamma$  peaks identified as arising from

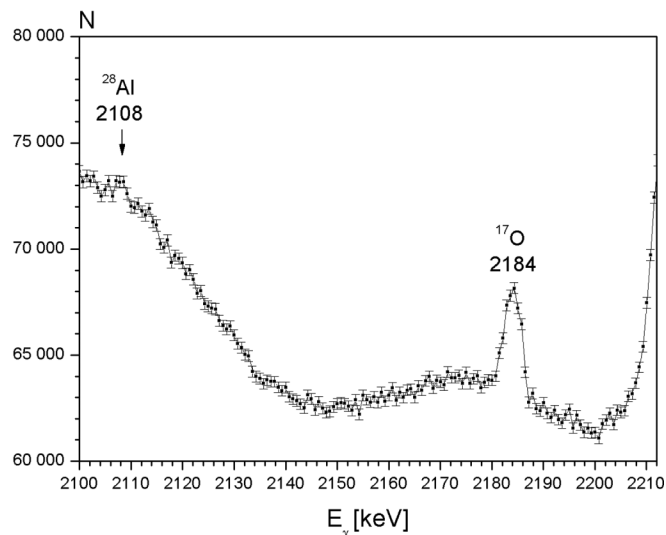


FIG. 4. Part of the  $\gamma$ -ray spectrum (2100–2210 keV) of the coaxial HPGe detector measured with the water target.

neutron capture by Ge isotopes in the coaxial HPGe detector and the BGO anti-Compton shield and assuming that these peaks were due to capture of cold neutrons scattered by the polyethylene target, we estimated the fluence of cold neutrons at the coaxial detector to be about  $\approx 10^5 \text{ cm}^{-2}$ .

In addition, as is known [29],  ${}^6\text{Li}$ -containing materials produce fast neutrons at energies of about 16 MeV after neutron capture by  ${}^6\text{Li}$  through the reactions

$$\begin{aligned} n({}^6\text{Li}, \alpha)t \quad (E_t = 2.73 \text{ MeV}); \quad t({}^6\text{Li}, {}^8\text{Be})n, \\ Q = 16.02 \text{ MeV}; \quad t({}^6\text{Li}, 2\alpha)n, \quad Q = 16.15 \text{ MeV} \quad (1) \end{aligned}$$

with probability  $\approx 10^{-4}$  per one thermal neutron captured by  ${}^6\text{Li}$  nuclei. As practically all cold neutrons scattered by targets are captured in the  ${}^6\text{Li}$  shielding, we estimate the total fluence of fast neutrons irradiating the HPGe detector as  $10^{14} \times 10^{-4} / 4 / 3.14 / 23.5^2 = 1.5 \times 10^6 / \text{cm}^2$ . Fast neutrons can produce numerous reactions of the types  $(n, n')$ ,  $(n, p)$ ,  $(n, \alpha)$ , and  $(n, 2n)$  in the HPGe detector and surrounding materials. Nuclear data concerning  $\gamma$  rays from nuclei produced as a result of these reactions are scarce. Therefore, it is not surprising that we found more than two dozen unidentified peaks in our  $\gamma$  spectra.

For purposes of more detailed analysis, the spectra and constraints on the search for two-photon transitions in the energy region of interest (2100–2210 keV) have been divided into several parts. For example, the spectrum in this energy range measured with the coaxial HPGe detector and polyethylene target (Fig. 2) was divided into five parts: 2100–2130, 2130–2152, 2152–2164, 2164–2180, and 2180–2210 keV. In each of these regions, the spectrum was described as a sum of polynomial functions up to third order,

$$N_1(E) = a_0 + a_1E + a_2E^2 + a_3E^3, \quad (2)$$

and Gaussian with  $\sigma$  corresponding to the HWHM  $\Delta = 1.3$  keV of the main peak with  $E = 2223$  keV:

$$N_2(E) = b_1 \exp\{-[(E - b_2)/\sigma]^2\}. \quad (3)$$

The least-squares MINUIT program [24] was used to determine constraints on the magnitude of possible  $\gamma$ -ray peak  $b_1$ .

The spectrum of the low-energy detector (Fig. 3) contains a peak with energy 2108.2 keV, identified as the  $\gamma$  transition in  ${}^{28}\text{Al}$  after neutron capture by  ${}^{27}\text{Al}$ , the sum of 2111.9 keV ( ${}^{74}\text{Ge}$ ), 2113.4 keV ( ${}^{57}\text{Fe}$ ), 2127.1 keV ( ${}^{74}\text{Ge}$ ), 2138.8 keV ( ${}^{28}\text{Al}$ ), and 2170.7 keV ( ${}^{28}\text{Al}$ ). The peak at 2163.5 keV did not find interpretation, but these peaks are hardly visible in the spectrum of the coaxial detector except for the weak peak at 2138.8 keV ( ${}^{28}\text{Al}$ ). Thus, the use of two detectors in the experiment permitted us to exclude the two- $\gamma$  cascade from  $np$  capture.

Figure 4 shows the spectrum in the energy range 2100–2210 keV measured with the water target.

The peak at 2184 keV is identified as due to neutron capture by  ${}^{16}\text{O}$  in water, and the weak peak at 2108 keV is from the  ${}^{28}\text{Al}$  nucleus. Their areas are in good agreement with the calculated ones. The first one takes into account the ratio of the neutron-capture cross sections by  ${}^{16}\text{O}$  and by protons in the water target and the 82% probability of the  $\gamma$  transition in  ${}^{17}\text{O}$ . The second ones compares its area with the areas of more intensive peaks from  ${}^{28}\text{Al}$  [25].

Using the same procedures for all spectra shown in Figs. 2–4, we obtained the final constraints  $R$  for the ratio of the magnitude of the searched-for second peak corresponding to the two-step  $\gamma$ -ray transition  ${}^3S_1$  (continuum)  $\rightarrow$   ${}^1S_0$  (metastable)  $\rightarrow$   ${}^3S_1$  (ground state) to the main transition  ${}^1S_0 \rightarrow$   ${}^3S_1$  with the energy 2223 keV,  $R < 6 \times 10^{-6}$ , and the cross section of the  $np$  capture followed by such a transition,  $\sigma < 2\mu\text{b}$  (two standard deviations).

## V. CONCLUSION

Our result implies that there is no evidence for the two-photon transition in the  $np$  capture with one of  $\gamma$  rays in the region 2100–2210 keV. The branching ratio is  $R < 6 \times 10^{-6}$  or cross section  $\sigma < 2\mu\text{b}$  (two standard deviations). This value is more than an order of magnitude less than prediction in Ref. [15]. Although this limit rejects the prediction of Ref. [15], it still leaves room for further investigation with lower background.

[1] J. M. Blatt and V. F. Weisskopf, *Theoretical Nuclear Physics* (John Wiley and Sons, New York, 1952).  
 [2] H. A. Bethe and P. Morrison, *Elementary Nuclear Theory*, 2nd ed. (John Wiley and Sons, London, 1956).  
 [3] S. T. Ma, *Rev. Mod. Phys.* **25**, 853 (1953).  
 [4] *Neutron Data Booklet*, edited by A.-J. Dianoux and G. Lander (Institut Laue-Langevin, Grenoble, France, 2002).  
 [5] B. L. Cohen, E. C. May, and T. M. O’Keefe, *Phys. Rev. Lett.* **18**, 962 (1967).  
 [6] B. L. Cohen, E. C. May, T. M. O’Keefe, and C. L. Fink, *Phys. Rev.* **179**, 962 (1969).  
 [7] W. Bohne, M. Hagen, H. Homeyer, H. Lettau, K. H. Maier, H. Morgenstern, and J. Scheer, *Phys. Rev. Lett.* **24**, 1028 (1970).  
 [8] N. O. Gaiser, S. E. Darden, R. C. Luhn, H. Paetz gen. Schieck, and S. Sen, *Phys. Rev. C* **38**, 1119 (1988).

[9] O. V. Bochkarev, A. A. Korshennikov, E. A. Kuzmin, I. A. Mukha, A. A. Ogloblin, L. V. Chulkov, and G. B. Yankov, *Yad. Fiz.* **46**, 12 (1987) [*Sov. J. Nucl. Phys.* **46**, 7 (1987)].  
 [10] N. Feather, *Nature (London)* **162**, 213 (1948); Z. Yingji, J. Dozhen, and Y. Jinqing, *Chin. Phys. Lett.* **6**, 113 (1989); K. K. Seth and B. Parker, *Phys. Rev. Lett.* **66**, 2448 (1991); D. V. Aleksandrov, E. Y. Nikolsky, B. G. Novatsky, D. N. Stepanov, and P. Volsky, *Pis’ma v ZhETF* **67**, 860 (1998); A. Spyrou, Z. Kohley, T. Baumann, D. Bazin, B. A. Brown, G. Christian, P. A. DeYoung, J. E. Finck, N. Frank, E. Lunderberg, S. Mosby, W. A. Peters, A. Schiller, J. K. Smith, J. Snyder, M. J. Strongman, M. Thoennessen, and A. Volya, *Phys. Rev. Lett.* **108**, 102501 (2012); F. M. Marqués, N. A. Orr, N. L. Achouri, F. Delaunay, and J. Gibelin, *ibid.* **109**, 239201 (2012); H. Witala and W. Glöckle, *Phys. Rev. C* **85**, 064003 (2012); M. Thoennessen, Z. Kohley,

- A. Spyrou, E. Lunderberg, P. A. DeYoung, H. Attanayak *et al.*, *Acta Phys. Pol. B* **44**, 543 (2013); E. S. Konobeevski, S. V. Zuyev, A. A. Kasparov, V. M. Lebedev, M. V. Mordovskoy, and A. V. Spassky, *Yad. Fiz.* **78**, 687 (2015); E. S. Konobeevski, *Phys. At. Nucl.* **78**, 643 (2015); I. Kadenko, *Europhys. Lett.* **114**, 42001 (2016).
- [11] J. E. Ungar *et al.*, *Phys. Lett. B* **144**, 333 (1984); F. M. Marques, M. Labiche, N. A. Orr, J. C. Angelique, L. Axelsson, B. Benoit, U. C. Bergmann, M. J. G. Borge, W. N. Catford, S. P. G. Chappell *et al.*, *Phys. Rev. C* **65**, 044006 (2002); D. V. Aleksandrov, E. Y. Nikolsky, B. G. Novatsky, S. B. Sakuta, and D. N. Stepanov, *Pis'ma v ZhETF* **81**, 49 (2005); K. Kisamori *et al.*, *Phys. Rev. Lett.* **116**, 052501 (2015); R. Y. Kezerashvili, [arXiv:1608.00169](https://arxiv.org/abs/1608.00169) [nucl-th].
- [12] J. Cerny, R. B. Weisenmiller, N. A. Jelley, K. H. Wilcox, and G. J. Wozniak, *Phys. Lett. B* **53**, 247 (1974); C. Detraz, *ibid.* **66**, 333 (1977); N. K. Timofeyuk, *J. Phys. G* **29**, L9 (2003); G. S. Anagnostatos, *Int. J. Mod. Phys. E* **17**, 1557 (2008); B. G. Novatsky, E. Y. Nikolsky, S. B. Sakuta, and D. N. Stepanov, *Pis'ma v ZhETF* **96**, 310 (2012).
- [13] K. Maltman and N. Isgur, *Phys. Rev. D* **29**, 952 (1984).
- [14] A. N. Ivanov, M. Cargnelli, M. Faber, H. Fuhrmann, V. A. Ivanova, J. Marton, N. I. Troitsakaya, and J. Zmeskal, [arXiv:nucl-th/0407079](https://arxiv.org/abs/nucl-th/0407079).
- [15] R. W. Hackenburg, Report BNL77483-2007-JA, Brookhaven Nat. Lab. Upton, New York, 2007.
- [16] T. Yamazaki, Y. Kuramashi, and A. Ukawa, *Phys. Rev. D* **84**, 054506 (2011).
- [17] S. B. Borzakov, JINR Comm. P15-89-430, Dubna, Russia, 1989.
- [18] S. B. Borzakov, *Jad. Fiz.* **57**, 517 (1994); *Phys. At. Nucl.* **57**, 488 (1994); JINR Comm. P15-93-29, Dubna, Russia, 1993.
- [19] A. A. Bergman, A. I. Isakov, Y. P. Popov, and F. L. Shapiro, *ZhETF* **33**, 9 (1957).
- [20] J. H. Gibbons and R. L. Macklin, *Phys. Rev.* **114**, 571 (1959).
- [21] S. B. Borzakov, N. A. Gundorin, L. B. Pikelner, N. V. Rebrova, and K. V. Zhdanova, *Proceedings of the ISINN-16*, Dubna, Russia, June 11–14, 2008 (JINR, Dubna, Russia, 2009).
- [22] S. B. Borzakov, N. A. Gundorin, and Y. N. Pokotilovski, *Phys. Part. Nuclei Lett.* **12**, 536 (2015).
- [23] Z. Revay, T. Belgya, Z. Kasztovszky, J. L. Weil, and G. L. Molnar, *Nucl. Instrum. Methods Phys. Res., Sect. B* **213**, 385 (2004).
- [24] <http://www.seal.web.cern.ch/seal/snapshot/work-packages/mathlibs/minuit/>.
- [25] <http://www.nndc.bnl.gov/CapGam/>; <http://www.nds.iaea.org>.
- [26] V. B. Zlokazov, *Nucl. Instr. Meth.* **199**, 509 (1982).
- [27] <http://www.canberra.com>.
- [28] <http://nucleardata.nuclear.lu.se/toi/radSearch.asp>.
- [29] M. A. Lone, D. C. Santry, and W. H. Inglis, *Nucl. Instrum. Methods Phys. Res., Sect. A* **174**, 521 (1980); V. Santoro, D. D. DiJulio, and P. M. Bentley, *J. Phys.: Conf. Ser.* **746**, 012012 (2016).